DYNAMICAL INTERACTIONS OF PLANETARY SYSTEMS IN DENSE STELLAR ENVIRONMENTS

JOHN M. FREGEAU, SOURAV CHATTERJEE, AND FREDERIC A. RASIO

Department of Physics and Astronomy, Northwestern University, 2145 Sheridan Road, Evanston, IL 60208;
fregeau@alum.mit.edu, s-chatterjee@northwestern.edu, rasio@northwestern.edu

ABSTRACT

We study dynamical interactions of star-planet binaries with other single stars. We derive analytical cross sections for all possible outcomes and confirm them with numerical scattering experiments. We find that a wide mass ratio in the binary introduces a region in parameter space that is inaccessible to comparable-mass systems, in which the nature of the dynamical interaction is fundamentally different from what has traditionally been considered in the literature on binary scattering. We study the properties of the planetary systems that result from the scattering interactions for all regions of parameter space, paying particular attention to the location of the "hard-soft" boundary. The structure of the parameter space turns out to be significantly richer than a simple statement of the location of the hard-soft boundary would imply. We consider the implications of our findings, calculating characteristic lifetimes for planetary systems in dense stellar environments and applying the results to previous analytical studies, as well as past and future observations. Since we recognized that the system PSR B1620−26 in the globular cluster M4 lies in the "new" region of parameter space, we performed a detailed analysis quantifying the likelihood of different scenarios in forming the system we see today.

Subject headings: celestial mechanics — globular clusters: general — methods: *n*-body simulations — planetary systems — pulsars: individual (PSR B1620−26)

Online material: color figure

1. INTRODUCTION

The subject of planets in dense stellar systems such as globular clusters came to life with the discovery that the binary pulsar PSR B1620−26 in the globular cluster M4 is orbited by a distant companion of approximately Jovian mass (Backer 1993; Thorsett et al. 1999; Sigurdsson et al. 2003 and references therein). The presence of such a system near the core of M4 is, at first, puzzling for several reasons. For example, the metallicity of M4 is low ($0.05 Z_\odot$), which makes the formation of such a planet via the standard core accretion model very unlikely and has sparked the creation of alternative formation theories (Beer et al. 2004 and references therein). In addition, the planet is on such a wide orbit about its host that the system should have been destroyed by dynamical interactions on a very short timescale ($\sim 10^8$ yr) in the moderately high density environment of M4's core, which implies that it must have been formed recently via an alternative mechanism such as a dynamical interaction involving a binary.

Campaigns searching for "hot Jupiter" planets (with orbital periods $\lesssim 10$ days) in 47 Tuc have yielded null detections, instead placing upper limits on the hot Jupiter frequency there (Gilliland et al. 2000; Weldrake et al. 2005). It now appears that the lack of hot Jupiters detected in 47 Tuc is probably more closely connected with the low metallicity of the environment and not simply due to destruction via dynamical encounters in the high-density stellar environment. This result is consistent with the strong correlation between host star metallicity and planet frequency in observed systems (Fischer & Valenti 2005). Searches for planets via transits in the higher metallicity environments of open clusters are currently under way.[1]

A key ingredient in the formation and evolution of planetary systems in dense stellar environments that is absent in lower density environments is dynamics. If either the stellar density is large enough or the planetary system is wide enough, it is likely to undergo a strong dynamical scattering interaction with another star or binary, perturbing its properties or possibly destroying it in the process. The importance of dynamics for wide mass ratio binaries cannot be overstated, especially when one considers the wealth of low-mass objects such as brown dwarfs that are known to exist in open and globular clusters and may be in binaries. In addition, the importance of dynamics as early as the stage of star formation is now becoming clear. There is now convincing evidence that a distant encounter with another star is responsible for the currently observed properties of distant solar system objects such as Sedna (Kenyon & Bromley 2004; Morbidelli & Levison 2004; Kobayashi et al. 2005). The object HD 188753 is a hierarchical triple star system composed of a main-sequence star in an ≈ 12.3 AU orbit about a compact main-sequence binary. What makes this system interesting is that the single star hosts a hot Jupiter in orbit about it, with a semimajor axis of ≈ 0.04 AU (Konacki 2005). The current configuration of the system is puzzling, since the binary companion would truncate the initial disk out of which the planet could have formed at a radius much smaller than that required by either the core accretion or gravitational fragmentation paradigms. It is now clear that the current configuration of HD 188753 must have resulted from a dynamical scattering interaction in a moderately dense stellar environment (Pfahl 2005; Portegies Zwart & McMillan 2005).

The types of dynamical interactions we have been discussing have been studied in great detail and volume since at least the mid-1970s for the case of comparable masses (Hills 1975; Heggie 1975; Heggie & Hut 2003 and references therein). The case of disparate masses in the binary (such as for a planetary system) has been treated in less detail (Hills 1984; Hills & Dissly 1989; Sigurdsson 1992), but with considerable attention paid to

---

[1] See http://star-www.st-and.ac.uk/~kdh1/transits/table.html.

TABLE 1

POSSIBLE OUTCOMES OF A DYNAMICAL SCATTERING INTERACTION BETWEEN
A PLANETARY SYSTEM, $[M_1\ m]$, AND A SINGLE STAR, M_2

Outcome	Description	Model Name
$[M_1\ m]\ M_2$	Preservation	"pres"
$[M_2\ m]\ M_1$	Exchange host star for incoming star	"ex_s"
$[M_1\ M_2]\ m$	Exchange planet for incoming star	"ex_p"
$M_1\ M_2\ m$	Ionization	"ion"
$[M_i:m\ M_j]$	Collision of planet with one star, resulting in a binary	
$M_i:m\ M_j$	Collision of planet with one star, resulting in ionization	
$[M_i:M_j\ m]$	Collision of two stars, resulting in a binary	
$M_i:M_j\ m$	Collision of two stars, resulting in ionization	
$M_i:M_j:m$	Collision of all objects	

NOTE.—Colons denote a physical collision.

the survivability of planetary systems in particular (Laughlin & Adams 1998; Bonnell et al. 2001; Davies & Sigurdsson 2001). To the best of our knowledge, there has not yet been a comprehensive treatment of dynamical scattering interactions with wide mass ratio systems in the literature, as previous work has typically been concerned with a numerical treatment of a certain aspect of the problem. This paper is an attempt to remedy this situation by carefully treating a wide area of parameter space both analytically and numerically and identifying physically distinct regions of the space, with an emphasis on application to physically interesting problems.

In particular, the questions we would like to answer in this paper are the following: For a dynamical interaction between a star-planet system and another star, under what conditions does the interaction result in (1) preservation of the planetary system, in the sense that the planet remains in orbit about its parent star, even if the orbit is perturbed; (2) exchange of the incoming star for the planetary system's host star; (3) destruction of the planetary system, in the sense that the planet is not bound to either star after the interaction; and (4) physical collisions involving two or more of the three objects? For the outcome in question 2, we would also like to know the resulting properties of the planetary system's orbit. In particular, we would like to know the regimes in which the planetary system orbit shrinks and those in which it widens.

In the language of binary scattering, the interaction of a binary planetary system with a single star can be written symbolically as "$[M_1\ m]\ M_2$," where the M_i represent the stars and m represents the planet. The possible outcomes can be enumerated succinctly as shown in Table 1. The outcome "pres" is preservation of the planetary system and can result either from a strong interaction or a weak flyby. The planetary system can have shrunk or widened in the process. The outcome "ex_s" is an exchange in which the host star of the planetary system is exchanged for the incoming star. The outcome "ex_p" is an exchange in which the two stars remain bound, ejecting the planet. The outcome "ion" leaves all objects (stars and planet) unbound from each other. The remaining outcomes listed in the table are various permutations involving one or more collisions. The outcome of a stable hierarchical triple is omitted from the table, since it is classically forbidden (Heggie & Hut 2003). It is possible for such a system to be formed as a result of a binary-single interaction if tidal effects are present. However, we ignore such effects in this paper.

Clearly, case 1 above corresponds to outcome "pres", case 2 corresponds to outcome "ex_s", and case 3 corresponds to outcomes "ex_p" and "ion". The outcomes corresponding to case 4 are the remaining ones listed in the table. In this paper we ad-

dress the questions posed above by calculating cross sections for the processes listed, as well as characteristic lifetimes. In § 2 we treat as much of the problem as we can analytically. In § 3 we confirm our analytical predictions with numerical experiments. In § 4 we determine under what conditions the planetary system will shrink or expand as the result of an exchange encounter, as well as the average amount by which it shrinks or expands. In § 5 we discuss the implications of the results in the context of the current literature and observations. In § 6 we quantify the likelihood of the possible dynamical formation scenarios of the planetary system PSR B1620−26 in the globular cluster M4. Finally, in § 7 we summarize and conclude.

2. ANALYTICAL CONSIDERATIONS

As described above, we symbolically label the interaction between a planetary system and a single star as "$[M_1\ m]\ M_2$." We also use the symbols M_i and m for the masses of the bodies, along with a for the planetary system semimajor axis, e for its eccentricity, v_∞ for the relative velocity at infinity between the planetary system and the single star, and b for the impact parameter. If one treats all bodies as point particles and only considers their masses for the time being, there are only two velocity scales in the problem. The first is what has historically been called the critical velocity, which is the value of v_∞ for which the total energy of the binary-single system is zero, and is given by

$$v_c = \left(\frac{GM_1 m}{\mu a}\right)^{1/2}, \qquad (1)$$

where $\mu = (M_1 + m)M_2/(M_1 + M_2 + m)$ is the reduced mass of the binary-single star system. The second is the orbital speed of the planet relative to its parent star, which is given by

$$v_{\mathrm{orb}} = \sqrt{\frac{G(M_1 + m)}{a}} \qquad (2)$$

for a circular orbit. If we look at equations (1) and (2), we see that if all the masses in the problem are comparable, then $v_c \approx v_{\mathrm{orb}}$. If, on the other hand, one of the members of the binary system is much less massive than the other member (as is the case for a planetary system), and we take $M_1 = M_2 \equiv M$ and $q \equiv m/M \ll 1$, then we can approximately write $v_c \approx \sqrt{q}v_{\mathrm{orb}}$. For a typical planetary system, $q \sim 10^{-3}$, and the two velocities differ by more than an order of magnitude. Figure 1 plots the two velocities for a planetary system with $q = 10^{-3}$ and $M = M_\odot$ as a function of a. In essence, introducing a mass ratio in the
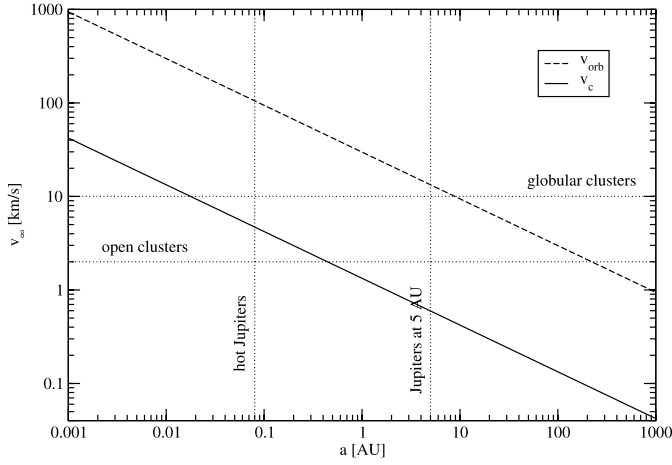
FIG. 1.—Plot of the critical velocity v_c and orbital speed v_{orb} for a planetary system composed of a 1 $M_\odot$ star and a 10^{-3} $M_\odot$ planet in an orbit with semimajor axis a, encountering a 1 $M_\odot$ star with relative velocity at infinity v_∞. Dotted lines represent characteristic velocity dispersions for open and globular clusters and orbital sizes for hot Jupiters and Jupiters at 5 AU, as shown.

binary opens up a strip in parameter space (between the two diagonal lines in Fig. 1) in which the physical character of dynamical scattering interactions is fundamentally different from that of the comparable-mass case.

In the literature on binary scattering involving stars of comparable mass, v_c is the velocity delimiting the border between "hard" and "soft" binaries (Heggie 1975). If $v_\infty < v_c$, the binary is in the hard regime and will on average harden (a will get smaller) as a result of an encounter. On the other hand, if $v_\infty > v_c$, the binary is in the soft regime and will on average soften (a will get larger) as a result of an encounter—that is, if the binary is not destroyed completely. However, Hills & Dissly (1989) and Hills (1990) suggest that when considering binaries with disparate masses, the boundary is more accurately given by $v_\infty = v_{orb}$, not by $v_\infty = v_c$, and they suggest the use of the terminology "fast-slow boundary" rather than "hard-soft boundary," since it is the relative speed of the binary members that is physically relevant. In the literature considering the survivability of planetary systems (and high mass ratio systems in general) in dense stellar environments, both v_c and v_{orb} have been used as the single characteristic velocity delimiting the boundary between ionization on the high-velocity side and hardening on the low-velocity side. However, as we will see below, for planetary systems the hard-soft boundary lies at $v_\infty = v_c$, while the characteristic timescale for the survivability of a planetary system in a dense environment drops markedly only at $v_\infty = v_{orb}$.

Now that we have written down the two characteristic velocities in the problem, thus dividing the parameter space into three distinct regions (as shown in Fig. 1), the question naturally arises: What is the physical character of the scattering interactions in each of the three regions? For $v_\infty < v_c$, the total energy of the binary-single system is negative. We thus expect that for any "strong" encounter (defined approximately as one in which the classical pericenter distance, r_p, between the single star and the planetary system is of order a), the interaction will be resonant, in the sense that it will survive for many orbital times (Heggie & Hut 2003). It will behave as a small star cluster, most likely ejecting its lightest member, in this case the planet, yielding the outcome "ex_p(res)". For $r_p \gtrsim a$, the likely outcome is a "direct" exchange of the incoming star for the planet ("ex_p(nonres)"). We thus expect $\sigma_{ex\_p} = \sigma_{ex\_p(res)} + \sigma_{ex\_p(nonres)}$ to be the dominant cross section for $v_\infty < v_c$. For $v_\infty > v_{orb}$, the

interaction is impulsive, since the timescale of the interaction is a small fraction of the binary orbital period. We thus expect that any "strong" interaction will ionize the system, making σ_{ion} the dominant cross section in this regime. For $v_c < v_\infty < v_{orb}$, the timescale of the interaction is comparable to the orbital period, so the outcome is not a priori obvious and must be treated numerically. Below, as far as it is possible, we calculate using analytical techniques the cross sections for each outcome in each of the three regions of parameter space.

2.1. $v_\infty < v_c$

First, since for $v_\infty < v_c$ the total energy of the binary-single system is negative, it is clear that ionization is classically forbidden. Thus,

$$\sigma_{ion} = 0. \tag{3}$$

We should also mention that for the outcome of preservation, the only method we have for determining if an interaction was "strong" is whether or not it was resonant. Thus, it should be clear that for every region of parameter space in Figure 1,

$$\sigma_{pres(nonres)} \to \infty, \tag{4}$$

since every very distant passage of the single star by the binary preserves it via a nonresonant interaction.

Heggie et al. (1996) considered interactions of "hard" binaries (in the sense that $v_\infty < v_c$) with single stars for a wide range of possible mass ratios in the binary and between the binary members and the incoming single star. Using analytical techniques, they calculated the scaling of the cross sections for each possible outcome. They then fitted to numerically calculated cross sections to determine the weakly mass-dependent "coefficients" on each cross section. From their equations (13) and (14), with $m_2 \approx m_3$ (since $M_1 \approx M_2$ here), we see that

$$\sigma_{ex\_p(res)} \approx \sigma_{ex\_p(nonres)}. \tag{5}$$

The cross section for nonresonant exchange of the planet for the incoming star is given by their equation (17) [divided by 2, since $\sigma_{ex\_p(res)} \approx \sigma_{ex\_p(nonres)}$]:

$$\sigma_{ex\_p(nonres)} \approx \frac{\pi G M_t a}{4 v_\infty^2} \left(\frac{M_1 + M_2}{M_t} \right)^{1/6} \left(\frac{M_2}{m + M_2} \right)^{7/2}$$
$$\times \left(\frac{M_1 + m}{M_t} \right)^{-1/3} \frac{M_2 + m}{M_t} \exp \left[\sum_{m,n} a_{mn} \left(\frac{m}{M_1 + m} \right)^m \left(\frac{M_2}{M_t} \right)^n \right], \tag{6}$$

where $M_t = M_1 + m + M_2$ is the total mass of the binary-single system, the exponential term is the "coefficient" fit to the numerical results, and the values of a_{mn} are given in their Table 3.

The cross section for direct exchange of the incoming star for the host star is also given by their equation (17), with the appropriate permutation of masses:

$$\sigma_{ex\_s(nonres)} \approx \frac{\pi G M_t a}{2 v_\infty^2} \left(\frac{M_2 + m}{M_t} \right)^{1/6} \left(\frac{M_2}{M_1 + M_2} \right)^{7/2}$$
$$\times \left(\frac{M_1 + m}{M_t} \right)^{-1/3} \frac{M_1 + M_2}{M_t} \exp \left[\sum_{m,n} a_{mn} \left(\frac{M_1}{M_1 + m} \right)^m \left(\frac{M_2}{M_t} \right)^n \right]. \tag{7}$$

The resonant cross section for this process, $\sigma_{\mathrm{ex\_s(res)}}$, can be calculated approximately by statistical techniques. Since for a resonant interaction we expect the three-body system to behave like a small star cluster, we can assume that the less massive body (the planet) and the more massive bodies (the stars) reach energy equipartition, yielding the approximate equality

$$mv_{\sigma,\,m}^2 = Mv_{\sigma,\,M}^2, \tag{8}$$

where $v_{\sigma,\,m}$ is the one-dimensional velocity "dispersion" of the planet, $v_{\sigma,\,M}$ is the one-dimensional velocity dispersion of the stars, and we let $M_1 = M_2 = M$. If we assume that the three-body system reaches thermal equilibrium on a timescale shorter than the interaction timescale, each species obeys a Maxwellian distribution:

$$f(v,\,n,\,v_\sigma) = 4\pi v^2 \frac{n}{(2\pi v_\sigma^2)^{3/2}} e^{-v^2/2v_\sigma^2}, \tag{9}$$

where n is the number density of the species, v_σ is its one-dimensional velocity dispersion, and v is its speed. To find the ratio of the probability for ejecting one of the stars to that for ejecting the planet, one simply integrates the velocity distribution for each species from the escape velocity, v_{esc}, to infinity and considers the ratio. By using the fact that $v_{\mathrm{esc}} \approx 2\sqrt{3}v_\sigma$, where $v_\sigma \approx v_{\sigma,\,M}$ is the one-dimensional velocity dispersion of the full three-object system, we have

$$
\begin{aligned}
\frac{\sigma_{\mathrm{ex\_s(res)}}}{\sigma_{\mathrm{ex\_p(res)}}} &= \frac{\int_{2\sqrt{3}v_\sigma}^{\infty} f(v,\,n,\,v_\sigma)\,dv}{\int_{2\sqrt{3}v_\sigma}^{\infty} f\left(v,\,n,\,\left(v_\sigma/\sqrt{q}\right)\right)\,dv} \\
&= \frac{2e^{-6}\sqrt{6/\pi} + \mathrm{erfc}\left(\sqrt{6}\right)}{2e^{-6q}\sqrt{6q/\pi} + \mathrm{erfc}\left(\sqrt{6q}\right)},
\end{aligned} \tag{10}
$$

where $\mathrm{erfc}(z) = 1 - \mathrm{erf}(z)$ is the complement of the error function. Note that there is no factor of 2 in the numerator, since the two stars in the system are distinguishable, in the sense that we distinguish between "ex_s(res)" and "pres(res)". This function is plotted in Figure 2. Note how, as q is decreased from unity, the test particle limit is reached relatively quickly, at $q \approx 0.1$. The same qualitative result is found in Fregeau et al. (2004), as shown in their Figure 10.

Since in a resonant interaction the system loses all memory of its initial configuration, we expect that for $M_1 = M_2 = M$, the probability of preserving the system (and ejecting the incoming star) in a resonant interaction is equal to that of ejecting the host star and keeping the incoming star:

$$\sigma_{\mathrm{pres(res)}} = \sigma_{\mathrm{ex\_s(res)}}. \tag{11}$$

Finally, we remark on the likelihood of collisions in this regime. Fregeau et al. (2004) have studied in detail the probability of collisions during binary interactions, including binaries with very small mass ratios, and have found that for systems in which the radius of the low-mass member is independent of its mass (as is approximately the case for planets), the test particle limit is reached at $q \approx 0.1$ (see Fig. 10 of that paper). In other words, the collision cross section is independent of the mass of the low-mass member below $q \approx 0.1$. Furthermore, the collision cross section is roughly as large as the strong interaction cross section. Therefore, we expect the combined cross section for any outcome involving a collision to be of the same order as $\sigma_{\mathrm{ex\_p(res)}}$. This estimate says nothing about the relative frequency of the different outcomes involving collisions, which requires numerical
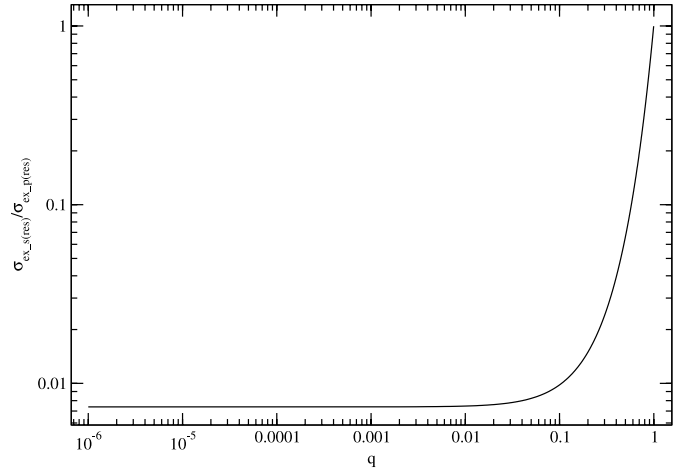

Fig. 2.—Plot of the ratio of the cross section for resonant exchange in which the planet's original host star is ejected, to that in which the planet is ejected, $\sigma_{\mathrm{ex\_s(res)}}/\sigma_{\mathrm{ex\_p(res)}}$, as a function of the binary mass ratio, $q \equiv m/M$. Here we have assumed that both stars have mass M. Note how, as q is decreased from unity, the test particle limit is reached relatively quickly, at $q \approx 0.1$.

calculations to infer, and which we do not treat in this paper. However, we do consider collisions briefly in the discussion of PSR B1620$-$26 in § 6.

2.2. $v_\infty > v_{\mathrm{orb}}$

In the regime in which $v_\infty > v_{\mathrm{orb}}$, since $v_\infty > v_c$, the total energy of the system is positive, so resonant scattering is forbidden:

$$\sigma_{\mathrm{pres(res)}} = \sigma_{\mathrm{ex\_s(res)}} = \sigma_{\mathrm{ex\_p(res)}} = 0. \tag{12}$$

Since $v_\infty > v_{\mathrm{orb}}$, the timescale of the scattering interaction is typically much smaller than the orbital period (unless $r_p \gg a$). In this case the interaction is in the impulsive limit and can be handled quite efficiently with analytical techniques (Hut 1983). From equation (5.1$'$) of Hut (1983), the ionization cross section is

$$\sigma_{\mathrm{ion}} = \frac{40}{3}\pi a G \frac{M_2^2}{M_1 + m}\frac{1}{v_\infty^2}. \tag{13}$$

Exchange in the impulsive regime occurs when the incoming star, M_2, passes much closer to one member of the binary than the other and undergoes a near-180° encounter in which all of its momentum is transferred to that member. In order for M_2 to remain bound in the binary, it must receive nearly zero recoil in the frame of the remaining binary member, which requires that the mass of M_2 be nearly equal to the mass of the binary member it displaces (Hut 1983). Thus, exchange of the planet for the incoming star, $\sigma_{\mathrm{ex\_p(nonres)}}$, is vanishingly small unless $M_2 \approx m$. Exchange of the planet's host star for the incoming star, on the other hand, is more likely, since the stars' masses are more likely to be comparable. From equation (5.2$'$) of Hut (1983), the cross section for exchange of the planet's host star for the incoming star is given by

$$\sigma_{\mathrm{ex\_s(nonres)}} = \frac{20}{3}\pi \frac{1}{a} G^3 M^2 (M + m)\frac{1}{v_\infty^6}, \tag{14}$$

with $M_1 = M_2 = M$.

2.3. $v_c < v_\infty < v_{\mathrm{orb}}$

In the regime $v_c < v_\infty < v_{\mathrm{orb}}$, the interaction is neither resonant nor impulsive, so the techniques used above cannot be used here.
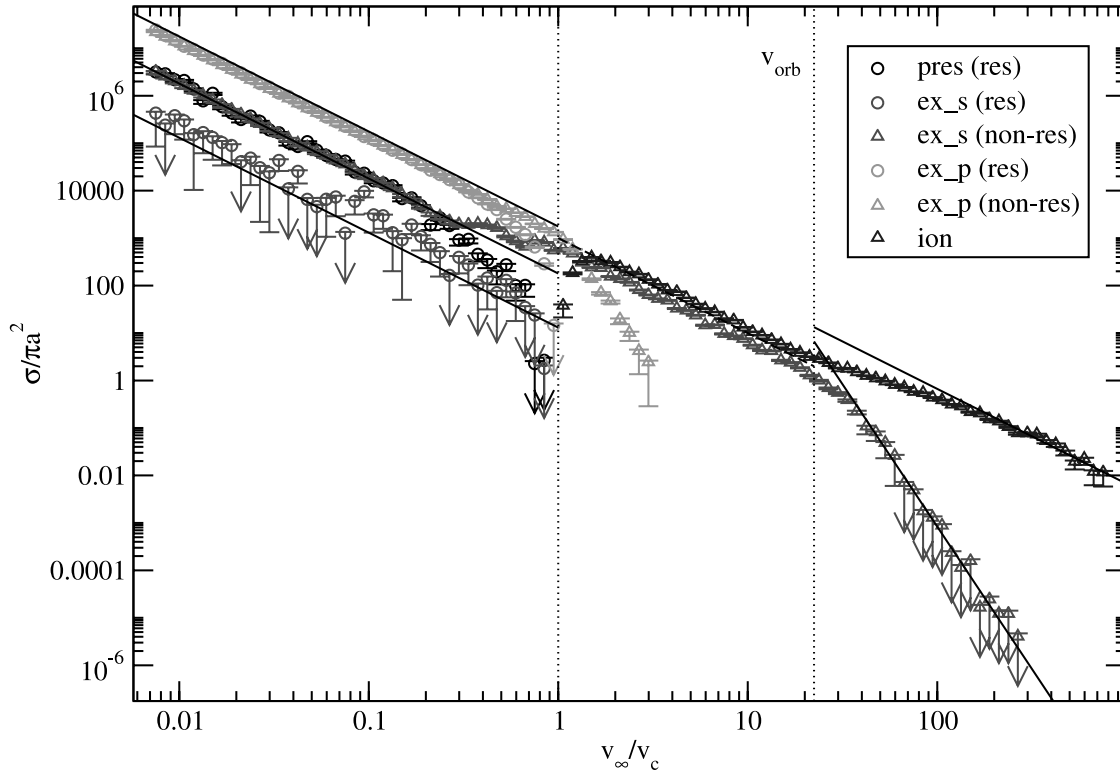
Fig. 3.—Dimensionless cross sections, $\sigma/\pi a^2$, for the outcomes involving no collisions in Table 1, as a function of v_∞/v_c for scattering interactions between a planetary system with mass ratio $q = m/M = 10^{-3}$ and eccentricity $e = 0$, and a star of mass M. Points plotted are as described in the legend. Circles represent resonant interactions, while triangles represent nonresonances ("direct" interactions). The error bars plotted are 1 σ. The vertical dotted lines represent the critical velocity and orbital speed. The solid lines show the analytically predicted cross sections from § 2, while the dashed line between the two vertical dotted lines indicates the order-of-magnitude estimated cross section from the same section. [See the electronic edition of the Journal for a color version of this figure.]

For $q \ll 1$ the interaction is essentially the hyperbolic restricted three-body problem, but since the timescale of the inter-action is of order a few orbital periods, the standard techniques of perturbation theory are of limited use. Instead, one must appeal to numerical methods to discern the nature of the interactions. It is possible, however, to make order-of-magnitude estimates of the relevant cross sections. Whenever M_2 passes within $r_p \lesssim a$ of the binary, its force on the planet is comparable to that of M_1, in which case the orbit of the planet should be sufficiently perturbed to unbind it from the host star and either eject it from the system or leave it bound to M_2. Thus, we estimate that the total cross section $\sigma_{ion} + \sigma_{ex\_s(nonres)}$ should be roughly equal to the strong interaction cross section. In the absence of any more detailed information, we simply assume $\sigma_{ion} \approx \sigma_{ex\_s(nonres)}$, yielding

$$\sigma_{ion} \sim \sigma_{ex\_s(nonres)} \sim \pi a \frac{GM_t}{v_\infty^2}, \qquad (15)$$

since gravitational focusing dominates. Since in this regime the planet is effectively a test particle, $\sigma_{ex\_p(nonres)}$ is vanishingly small.

3. NUMERICAL CONFIRMATION

To confirm the analytical predictions of § 2, we have calcu-lated the cross sections by numerically integrating many scatter-ing interactions. We have used the Fewbody numerical toolkit to perform the scattering interactions (Fregeau et al. 2004). For cal-culating the cross sections, we use a generalization of the tech-nique described in McMillan & Hut (1996), in which, for each annulus in impact parameter, we perform only one scattering interaction instead of the many required by their technique. This allows us to more precisely calculate the uncertainties in the

cross sections, in particular yielding accurate asymmetric error bars. To handle the small number statistics, we use the tables in Gehrels (1986).

Figure 3 shows the dimensionless cross sections, $\sigma/\pi a^2$, for the outcomes involving no collisions in Table 1, as a function of v_∞/v_c for a planetary system with mass ratio $q = 10^{-3}$, $e = 0$, and $M_1 = M_2 = M$. Points plotted are as described in the legend. Circles represent resonant interactions, while triangles represent nonresonances ("direct") interactions. The error bars plotted are 1 σ. The vertical dotted lines represent the critical velocity and orbital speed. The solid lines show the analytically predicted cross sections from § 2, while the dashed line between the two vertical dotted lines indicates the order-of-magnitude estimated cross sec-tion from the same section. We have calculated the same cross sec-tions using Starlab (McMillan & Hut 1996; Portegies Zwart et al. 2001), and the agreement is excellent. Note that with the excep-tion of those in § 6, all calculations presented in this paper are per-formed with $e = 0$. Previous results show that most cross sections of interest do not depend strongly on eccentricity (Hut & Bahcall 1983). Indeed, we have calculated the cross sections in Figure 3 using a thermal eccentricity distribution and find only a slight increase in the resonant cross sections (and a corresponding de-crease in the nonresonant cross sections) relative to the $e = 0$ case.

If we look first at the region in which $v_\infty > v_{orb}$, we see σ_{ion} plotted with dark gray triangles and $\sigma_{ex\_s(nonres)}$ plotted with me-dium gray triangles, along with the corresponding analytically predicted cross sections (eqs. [13] and [14], respectively), which are plotted as solid lines. The agreement is clearly quite excellent.

Next, if we look at the region in which $v_\infty < v_c$, we see $\sigma_{ex\_p(res)}$ (circles) and $\sigma_{ex\_p(nonres)}$ (triangles) plotted in light gray, with the corresponding analytically predicted result of equation (6) (the
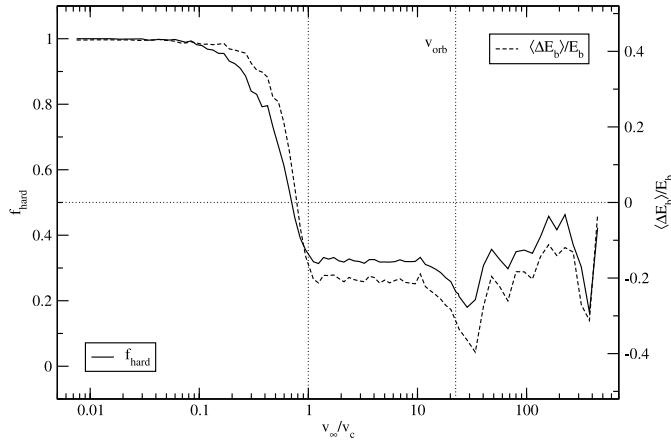
Fig. 4.—Statistics on the final planetary systems formed via nonresonant exchange in which the planet's original host star is ejected ("ex_s(nonres)"), as a function of v_∞/v_c, for the case with $M_1 = M_2 = M$ and $q = 10^{-3}$. The fraction of final planetary systems that have hardened (semimajor axis decreased), f_{hard}, is shown by the solid line. The average change in the binding energy of the planetary system, $\langle\Delta E_b\rangle/E_b = \langle GMm/2a' - GMm/2a\rangle/(GMm/2a) = a\langle 1/a'\rangle - 1$, is shown by the dashed line. The vertical dotted lines represent the critical velocity and the orbital speed. The horizontal dotted line represents the value 0.5 for f_{hard} and 0 for $\langle\Delta E_b\rangle/E_b$. The hard-soft boundary lies where f_{hard} crosses 0.5 and $\langle\Delta E_b\rangle/E_b$ crosses 0, which clearly and robustly occurs at $v_\infty \approx 0.75 v_c$.

two cross sections are expected to be roughly equal, from eq. [5]) plotted as a solid line. The values of $\sigma_{\mathrm{ex\_p(res)}}$ and $\sigma_{\mathrm{ex\_p(nonres)}}$ appear to be roughly equal, with those of $\sigma_{\mathrm{ex\_p(res)}}$ larger by $\sim$10% for $v_\infty \ll v_c$, while the analytical prediction is roughly $\sim$50% larger than the numerical result. Plotted with medium gray triangles is $\sigma_{\mathrm{ex\_s(nonres)}}$, along with the corresponding analytical result from equation (7), which is also plotted as a solid line. Clearly the agreement is superb. Plotted with medium gray circles is the resonant cross section $\sigma_{\mathrm{ex\_s(res)}}$, with the analytical result from equation (10) plotted as a third solid line. Although the statistics on this very small cross section are not as good as those for the other cross sections in $v_\infty < v_c$, it still appears to agree very well with the analytical prediction. Finally, plotted with black circles is $\sigma_{\mathrm{pres(res)}}$. Although from equation (11) above we would expect it to be equal to $\sigma_{\mathrm{ex\_s(res)}}$, it is larger by nearly an order of magnitude. The discrepancy is due to the operational definition of resonance we have used; namely, that the mean-squared separation of all bodies makes more than one minimum, with a successive minimum counted only if the intervening maximum between it and the previous minimum is at least twice the value of both minima (McMillan & Hut 1996). Clearly this definition is too liberal and classifies some preservation outcomes as resonant when they should not be classified as such. In fact, requiring that the mean-squared separation make more than two minima for a resonance decreases $\sigma_{\mathrm{pres(res)}}$ by about an order of magnitude, bringing it into agreement with the analytical prediction and making it nearly equal to $\sigma_{\mathrm{ex\_s(res)}}$. Requiring that intervening maxima be 4 times (instead of twice) the value of the minima on either side for a successive minimum to be counted has no discernible effect on the results.

In the region in which $v_c < v_\infty < v_{\mathrm{orb}}$, resonance is, of course, forbidden. The cross section $\sigma_{\mathrm{ex\_p(nonres)}}$ drops off quickly above $v_\infty = v_c$, obeying roughly

$$\frac{\sigma_{\mathrm{ex\_p(nonres)}}}{\pi a^2} \approx \left(1.5 \times 10^3\right)\left(\frac{v_\infty}{v_c}\right)^{-6} \qquad (16)$$

for the case in which $M_1 = M_2 = M$ and $q = m/M = 10^{-3}$. The cross sections for ionization and exchange of the incoming star

for the host star (plotted with dark gray and medium gray triangles, respectively) are of the same order of magnitude and are only slightly different from the order-of-magnitude estimate in equation (15) (dashed line). In particular, for the bulk of the region, $\sigma_{\mathrm{ion}} \approx 2\sigma_{\mathrm{ex\_s(nonres)}}$, and σ_{ion} is $\sim$20% larger than the order-of-magnitude estimate, yielding

$$\sigma_{\mathrm{ion}} \approx 1.2\pi a \frac{GM_t}{v_\infty^2} \qquad (17)$$

and

$$\sigma_{\mathrm{ex\_s(nonres)}} \approx 0.6\pi a \frac{GM_t}{v_\infty^2}, \qquad (18)$$

again, for the case in which $M_1 = M_2 = M$ and $q = m/M = 10^{-3}$. However, as discussed above in § 2, we expect the test particle limit to be reached at $q \approx 10^{-1}$, so the results here should be valid for all values of $q \lesssim 10^{-1}$.

4. PROPERTIES OF EXCHANGE SYSTEMS AND THE HARD-SOFT BOUNDARY

Now that we have determined the character of the scattering interactions in each region of parameter space shown in Figure 1, we consider the properties of the final planetary system for the outcomes that yield a planetary system, namely, resonant preservation, and exchange of the host star for the incoming star. Since resonance is only allowed for $v_\infty < v_c$, for simplicity we consider only the outcome "ex_s(nonres)", which has a significant cross section for all values of v_∞. Shown in Figure 4 are the statistical properties of the final planetary systems in the outcome "ex_s(nonres)" as a function of v_∞/v_c, for the case with $M_1 = M_2 = M$, $q = 10^{-3}$, and $e = 0$. The fraction of the final planetary systems that have hardened (semimajor axis decreased), f_{hard}, is shown by the solid line. The average change in the binding energy of the planetary system,

$$\langle\Delta E_b\rangle/E_b = \langle GMm/2a' - GMm/2a\rangle/(GMm/2a) = a\langle 1/a'\rangle - 1,$$

is shown by the dashed line. The vertical dotted lines show the critical velocity and the orbital speed. The horizontal dotted line represents the value 0.5 for f_{hard} and 0 for $\langle\Delta E_b\rangle/E_b$. For $v_\infty \ll v_c$, every outcome results in the planetary system hardening, with $\langle\Delta E_b\rangle/E_b \approx 0.4$. This implies that the semimajor axis has shrunk to about 70% of its initial value, as shown in Figure 5, which plots $\langle a/a'\rangle^{-1}$ as a function of v_∞/v_c. In the region in which $v_c < v_\infty < v_{\mathrm{orb}}$, the planetary system predominantly widens as a result of the encounter, with only $\approx$30% of systems hardening. The systems do not widen by much, on average decreasing their energy by about 20%. This corresponds to an increase in the semimajor axis of about 25%, as shown in Figure 5. This is rather interesting, since in this region exchange is nearly as likely as ionization, implying that a significant fraction of systems that undergo a strong dynamical encounter survive it. Furthermore, those that survive suffer a comparatively small change in their semimajor axis, with a significant fraction actually hardening. Finally, in the region in which $v_\infty > v_{\mathrm{orb}}$, since the cross section for ionization is several orders of magnitude larger than that of exchange, the statistics are too poor to say anything conclusive. Although the curves in Figures 4 and 5 appear to begin to rebound, we expect that they actually go smoothly to $f_{\mathrm{hard}} = 0$, $\langle\Delta E_b\rangle/E_b = -1$, and $\langle a/a'\rangle^{-1} \to \infty$.

As was described in § 2, there has been considerable variance in the literature on what velocity demarcates the hard-soft boundary
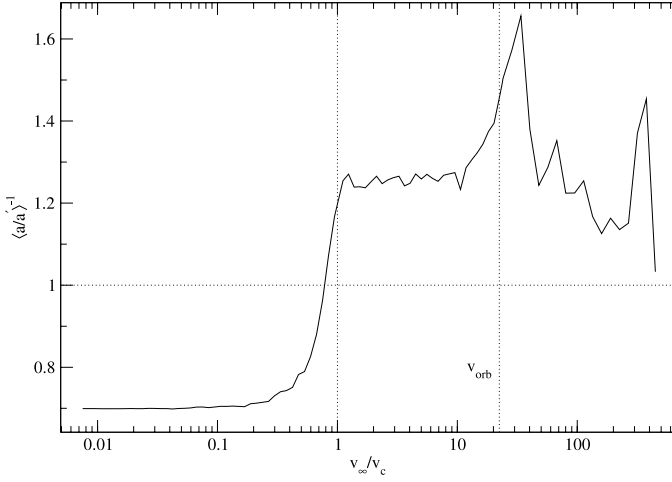
FIG. 5.—Plot of the quantity $\langle a/a' \rangle^{-1}$, the inversely weighted average of the ratio of the planetary system's final semimajor axis a' to its initial value a, as a function of v_∞/v_c for the planetary systems formed via nonresonant exchange in which the planet's original host star is ejected ("ex_s(nonres)"), for the case with $M_1 = M_2 = M$ and $q = 10^{-3}$. The vertical dotted lines show v_c and v_{orb}, while the horizontal dotted line shows the value 1 for $\langle a/a' \rangle^{-1}$.
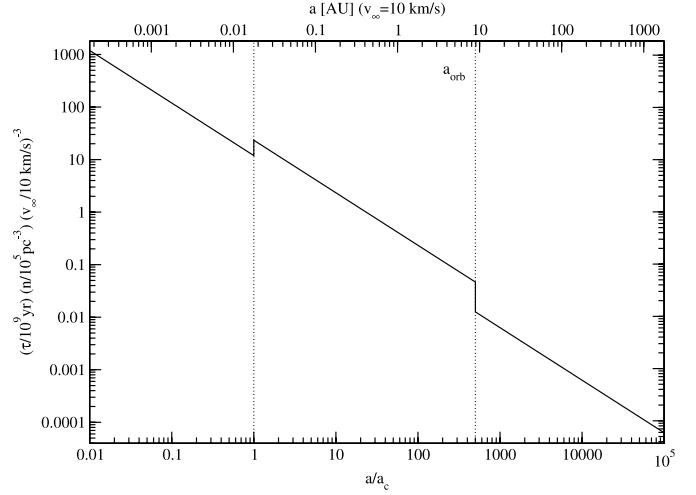

FIG. 6.— Characteristic lifetime τ, plotted in the quantity $\tau n/v_\infty^3$ (see eq. [22]), of a planetary system with mass ratio $q = 10^{-3}$, host star mass $M = M_\odot$, and eccentricity $e = 0$ in a stellar environment of number density n and velocity dispersion v_∞, as a function of a/a_c. The critical semimajor axis a_c is as defined in § 4 after eq. (22). The two vertical dotted lines show $a = a_c$ and $a = a_{orb}$. The quantity a_{orb} is the value of a for which the orbital speed in the planetary system is equal to v_∞.

for systems with a wide mass ratio. A look at Figure 4 reveals that (at least for $M_1 = M_2$) the hard-soft boundary, which lies where f_{hard} crosses 0.5 and $\langle \Delta E_b \rangle / E_b$ crosses 0, robustly occurs at $v_\infty \approx 0.75 v_c$. Of course, simply stating that the hard-soft boundary lies at $v_\infty \approx 0.75 v_c$ belies the fact that for $v_c < v_\infty < v_{orb}$ the likelihood of a planetary system surviving a strong dynamical encounter in some form is rather significant.

On the basis of the understanding garnered from our analysis thus far, it is useful to consider the fate of a planetary system subject to strong dynamical encounters in a stellar environment of number density n and velocity dispersion v_σ. The average relative velocity between objects in such a system is roughly $\sqrt{2} v_\sigma$, but since we are interested only in orders of magnitude here, we will take $v_\infty = v_\sigma$. Since we know all relevant cross sections, we can perform a simple "$n\sigma v$" estimate for the lifetime of a planetary system as a function of a,

$$\tau = \frac{1}{n\sigma v_\infty}, \qquad (19)$$

which we do now. A useful way to think about the evolution of a planetary system subject to encounters is the following. If we take the masses to be given, then for a given value of a we know v_c and v_{orb} from equations (1) and (2). Given the value of v_∞ fixed by the velocity dispersion of the stellar environment in which the planetary system finds itself, we thus have v_∞/v_c and know in which section of parameter space the planetary system lies in Figure 3. In the region in which $v_\infty < v_c$, by far the most likely outcome of a strong dynamical interaction is an exchange in which the planet is ejected. Thus, the value of τ for this region can be calculated using the cross section $\sigma_{ex\_p} = \sigma_{ex\_p(res)} + \sigma_{ex\_p(nonres)}$. In the region in which $v_\infty > v_{orb}$, the dominant outcome is ionization, so one uses σ_{ion} in equation (19). In between, in the region in which $v_c < v_\infty < v_{orb}$, the outcomes "ion" and "ex_s(nonres)" are almost equally likely. From equations (17) and (18), roughly $X_i \equiv 2/3$ of strong dynamical interactions result in ionization, while the remaining $X_e \equiv 1/3$ result in nonresonant exchange of the host star for the incoming star. The systems that undergo exchange suffer only a small perturbation to their orbital size, as evidenced by Figure 5. As a changes, v_c and v_{orb} scale as $a^{-1/2}$ with v_c/v_{orb} fixed. Thus, in effect, as a changes, the quantity

v_∞/v_c scales as $a^{1/2}$ with the distance between v_c and v_{orb} held fixed in logarithmic space, and so the planetary system simply occupies a new position on the x-axis in Figure 3. A planetary system lying in regions in which $v_\infty < v_c$ or $v_\infty > v_{orb}$ is destroyed as a result of an interaction. But for a planetary system in the intermediate region, it is destroyed a fraction X_i of the time, while the other fraction X_e of the time it survives with v_∞/v_c increased by a mere $\sim$10% on average (from Fig. 5). Eventually, systems that survive via many exchange interactions will find themselves in the region in which $v_\infty > v_{orb}$ and will be destroyed quickly by ionization. Since the average change in a due to these exchanges is rather small, let us, for the sake of simplifying the calculation of τ, assume that they survive indefinitely. The average lifetime in this region of parameter space, including both ionization and exchange, is thus

$$\tau = \tau_i + X_e \tau_i + X_e^2 \tau_i + X_e^3 \tau_i + \cdots = \frac{\tau_i}{1 - X_e}, \qquad (20)$$

where

$$\tau_i = \frac{1}{n \left(\sigma_{ion} + \sigma_{ex\_s(nonres)} \right) v_\infty}. \qquad (21)$$

Since all cross sections of interest here scale as $\sigma = \sigma_0 a / v_\infty^2$, where σ_0 is a function of the masses, we can be quite general and plot

$$\frac{\tau n}{v_\infty^3} = \frac{1}{\sigma_0} \left(\frac{a}{a_c} \right)^{-1} \frac{\mu}{GM_1 m}, \qquad (22)$$

where the critical semimajor axis is $a_c = GM_1 m/\mu v_\infty^2$, as a function of a/a_c in Figure 6. Note that the sharpness of the transitions at $a = a_c$ and $a = a_{orb}$ is due to the use of the analytical cross sections in calculating the lifetimes. From the numerical cross sections in Figure 3 it is evident that, in reality, the transitions are a bit smoother, although the general structure is the same. Clearly, the overall trend is for the lifetime to scale as a^{-1}, with the coefficient varying by only a factor of a few among the different regions of parameter space. Using only the fact that the

hard-soft boundary lies at $v_\infty = v_c$, one might expect the lifetime to drop markedly at $a = a_c$. In fact, it increases slightly there and does not drop until $a = a_{\mathrm{orb}}$, due to the large cross section for planetary systems preserving exchange in the intermediate regime. We now consider the implications of this result.

5. IMPLICATIONS

The main implication of our results is that the minimum size of planetary systems that will likely be destroyed as a result of dynamical interactions in dense stellar environments is larger than has previously been assumed. This limit can be read almost directly from Figure 6 for a given velocity dispersion, stellar density, and timescale. For example, in a globular cluster like 47 Tuc, which has a central stellar density of $\sim 10^5$ pc^{-3} and a velocity dispersion of ~ 10 km s^{-1}, planetary systems wider than 0.05 AU will have been destroyed after ~ 10 Gyr. The second implication is that the statement that the location of the hard-soft boundary is at $v_\infty = v_c$, although correct, when taken on its own can be misleading. It is true that planetary systems on the low-velocity side of the hard-soft boundary that survive interactions tend to harden on average. However, planetary systems are overwhelmingly likely to be destroyed in this regime, as can be read directly from the cross sections in Figure 3. Similarly, although planetary systems tend to soften, on average, for $v_\infty > v_c$, it is not until $v_\infty > v_{\mathrm{orb}}$ that ionization dominates the outcome. In other words, there is a wide region in parameter space (from $v_\infty = v_c$ to $v_\infty = v_{\mathrm{orb}}$) for which the probability of exchange in which a planetary system results is comparable to that of ionization, and those resulting planetary systems soften by only a small amount (as shown in Figs. 4 and 5).

Our results have a bearing on previous studies in the literature in which authors have adopted inappropriate prescriptions for outcomes of scattering interactions with planetary systems. As an example, Bonnell et al. (2001) calculated the evolution of a population of planetary systems in stellar environments of differing density, using a Monte Carlo approach in which planetary systems undergo binary-single interactions with field stars. As a result of each interaction, the planetary system is assumed to be ionized if $v_\infty > v_c$ and to harden if $v_\infty < v_c$. However, as our results show, for $v_\infty < v_c$ those planetary systems undergoing strong interactions are destroyed, for $v_c < v_\infty < v_{\mathrm{orb}}$ they have an increased probability of surviving, and for $v_\infty > v_{\mathrm{orb}}$ they are predominantly ionized. The result of the discrepancy is that most of the systems destroyed on the high-velocity side of the hard-soft boundary ($v_\infty = v_c$) in these simulations will actually survive as planetary systems of some kind. The growth of a spike in the relative frequency of planetary systems smaller than a_c predicted in low-velocity dispersion systems (such as open clusters) should not occur, with the distribution of semimajor axes dropping smoothly from a_c to a_{orb}. There is the possibility for a slight hump in the relative frequency of planets with $a_c < a < a_{\mathrm{orb}}$, on the basis of our Figure 6, but it would not be nearly as pronounced as what is shown in Figure 5 of Bonnell et al. (2001).

On the observational side, we find that, of the hot Jupiter planetary systems expected to be detected in 47 Tuc in the transit survey of Gilliland et al. (2000), which was sensitive to periods of up to ≈ 4 days, essentially all are expected to survive dynamical interactions in the high-density core of the cluster on timescales comparable to the age of the cluster. This can be read directly from Figure 6 with $a \approx 0.05$ AU. This bolsters the conclusion drawn by Weldrake et al. (2005) that it is not dynamics that is responsible for the lack of hot Jupiters detected in 47 Tuc,

but rather may be metallicity-dependent effects (Fischer & Valenti 2005). The Weldrake et al. study sampled regions outside the core and was sensitive to orbital periods up to ≈ 16 days, so the hot Jupiter binaries that they looked for would also not have been destroyed by dynamical interactions due to the lower density there. However, it is possible that they would have been destroyed early in the lifetime of the cluster if it went through a high-density phase early on, the possibility of which is discussed in Bonnell et al. (2001).

Looking ahead, we now speculate on future possibilities for observations of planets in dense stellar environments. The globular cluster Terzan 5 is unique in that it has supersolar metallicity. Any argument against the formation of planets in globular clusters due to metallicity effects is null in Terzan 5. If we adopt the frequency of hot Jupiters in the solar neighborhood of 0.8% (Butler et al. 2000; Basri 2004) and use the estimated central number density of 10^5 pc^{-3} and core radius of 0.5 pc (Harris 1996), we would expect ~ 100 hot Jupiters to be in orbit around main-sequence stars in the core of Terzan 5. According to Figure 6, for $v_\infty = 10$ km s^{-1}, all of these systems would survive for a Hubble time, since the definition of a "hot Jupiter" implies an orbit period of less than ~ 10 days. Terzan 5 lies nearly in the Galactic disk, close to the Galactic center, making optical observations of it practically impossible. However, it is readily observed in radio wavelengths, and already many millisecond pulsars (MSPs) have been discovered in it (Ransom et al. 2005). There is thus the possibility of detecting planets in orbits around MSPs in this cluster. The most natural formation mechanism involves exchanging the MSP for the planet's host star in a dynamical interaction. From Figure 1 we see that, for the velocity dispersion of Terzan 5, planetary systems with $a \sim 0.01 - 10$ AU lie in the intermediate regime and are thus most likely to possibly have brought in a MSP through exchange. The formation of such systems is a balancing act between destruction (for the wider systems) and a long interaction timescale (for the smaller systems), with a "sweet spot" at $a \sim 0.1$ AU. Although the expected number of MSP-planet systems is small (probably ~ 1), we can predict that such a system would have $a \sim 0.1$ AU. There is also the possibility that planets could form around pulsars, but the frequency of formation is rather less certain (Sigurdsson 1992).

6. PSR B1620−26

The planetary system PSR B1620−26 in the globular cluster M4 consists of a Jovian-mass object in an ≈ 20 AU orbit about a MSP−white dwarf (WD) binary. The planetary system sits right at the edge of the core of M4 in projection, which has a central velocity dispersion of ≈ 4 km s^{-1}. If we look at Figure 1, we see that the planetary system lies comfortably in the "intermediate" regime, making it very likely that it was formed via a dynamical scattering interaction in which the neutron star−containing (NS-containing) binary exchanged into the planetary system (as one unit) in place of the planet's original host star (scenario 2 below). With this motivation, we now perform a detailed numerical analysis of the possible formation scenarios of PSR B1620−26.

First, it is useful to list the physical parameters of the system. The pulsar has a spin period of ≈ 11 ms and a mass of $\approx 1.35\ M_\odot$, while the WD has a mass of $0.34 \pm 0.04\ M_\odot$. *Hubble Space Telescope* data have confirmed that the WD is young, with an age of ~ 0.5 Gyr. The PSR-WD binary has an eccentricity of ~ 0.025. The planet has a mass of $\approx 1 - 3 M_{\mathrm{J}}$, where M_{J} is the mass of Jupiter, and orbits with an eccentricity of ~ 0.3 about the MSP-WD binary. The inclination between the inner and outer orbits is $\sim 55^{+14}_{-8}$ deg. The currently favored dynamical formation scenarios are the following. In what we will call scenario 1 a binary

composed of a WD and a NS undergoes an exchange interaction with a binary consisting of a main-sequence star near the turn-off mass and a Jovian planet. In the encounter the WD is ejected from the system, with the normal star exchanging into orbit with the PSR, which leaves the planet in a wide orbit about the star-PSR binary. The star then undergoes mass transfer as it goes through the red giant phase, recycling the PSR to millisecond periods (Sigurdsson et al. 2003). In scenario 2, a binary composed of a NS and a near–turn-off main-sequence star of mass 0.8 $M_\odot$ undergoes an exchange interaction with a binary composed of a main-sequence star and a Jovian planet. In the encounter the NS-star binary acts as a single unit and exchanges into the planet's orbit, ejecting the planet's original host star. The star then undergoes mass transfer as it goes through the red giant phase, recycling the PSR to millisecond periods (Ford et al. 2000). As we discuss below, our expectation that scenario 2 is the much more likely one proved to be correct.

6.1. *Quantifying the Outcome Likelihoods*

As in § 3, we use the Fewbody numerical toolkit to perform scattering interactions and calculate cross sections for different outcomes. The interaction rate per planetary system is simply

$$R = \int_0^\infty dv_\infty \, f(v_\infty) n \sigma v_\infty, \qquad (23)$$

where $f(v_\infty)$ is the velocity distribution function, n is the number density of NS binaries, and σ is the cross section for the outcome of interest. Rates presented below were calculated by discretizing the integral over the distribution function and summing over a range of velocities wide enough to guarantee convergence. In particular, we typically integrate over a range of velocities from 1 to 15 km s^{-1}, with the upper limit set by the escape speed of 15.25 km s^{-1} of the cluster (Beer et al. 2004). For the distribution function we assume a simple Maxwellian with a velocity dispersion of $v_\infty = \sqrt{2} v_\sigma$, where $v_\sigma = 3.88$ km s^{-1} is the velocity dispersion in the core of M4 and the factor of $\sqrt{2}$ is due to the fact that we are considering relative velocities between pairs of objects. Our naming convention for the objects is analogous to what we used above, with "[NS MS1] [MS2 P]" denoting the initial configuration of the two binaries before the scattering interaction. "MS1" in fact represents a WD in scenario 1 and a main-sequence star in scenario 2; however, we label it "MS1" in both cases since it is only the mass of the object that matters in the scattering interactions (the radius of the object plays only a minor role when direct physical collisions are considered). We label the semimajor axis of the NS-MS1 binary a_0 and that of the MS2-P binary a_1. Since the NS binary must be significantly tighter than the planet binary, it is expected to behave dynamically as a single unit; thus, the cross sections for different outcomes are expected to scale with a_1 (our numerical results confirm this). We therefore vary only a_0, from 0.1 to 1 AU (a typical range of values), and keep a_1 fixed at 5 AU. We fix e_1, the eccentricity of the planet binary, at 0, while we draw e_0, the eccentricity of the NS binary, from a thermal distribution truncated at large e_0 such that neither object in the binary exceeds its Roche lobe. Figure 7 shows the seminormalized rate $R/[n\pi(a_0 + a_1)^2]$ (in units of km s^{-1}) for the different outcomes listed in the legend as a function of a_0. The most likely outcome is [NS MS1] MS2 P; that is, destruction of the planetary system and preservation of the NS binary. The next most likely outcome is scenario 2 ([[NS MS1] P] MS2), confirming our expectations from above. The next is any outcome involv-
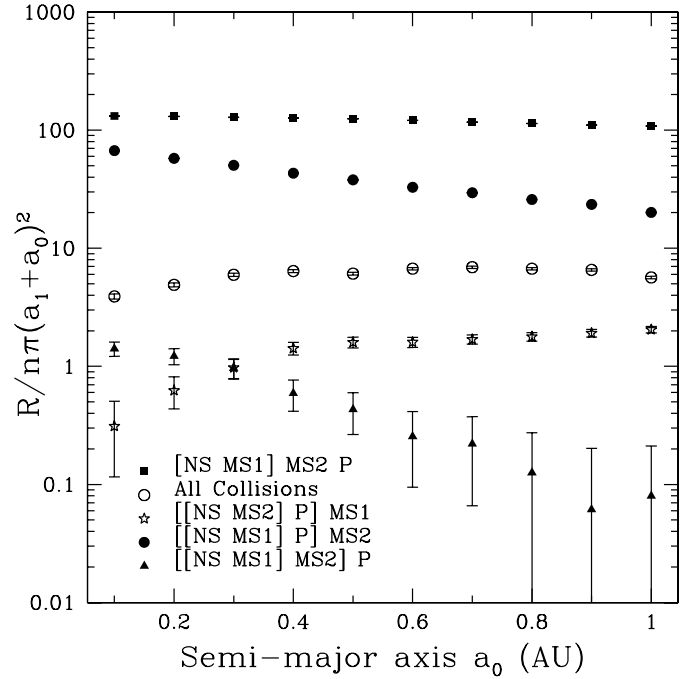

Fig. 7.—Quantifying the likelihood of the possible formation scenarios of PSR B1620−26: Plot of the seminormalized rate $R/[n\pi(a_0 + a_1)^2]$ (in units of km s^{-1}) for various outcomes of a scattering interaction between a NS-MS1 binary and a MS2-P planetary system as a function of a_0, the semimajor axis of the NS-MS1 binary. Symbols are as defined in the legend. The rate for scenario 2 ([[NS MS1] P] MS2) clearly dominates over scenario 1 ([[NS MS2] P] MS1) for a wide range in values of a_0.

ing direct physical collisions between system members, which we lump together into one category for the sake of succinctness. The next is scenario 1 ([[NS MS2] P] MS1), which is larger than [[NS MS1] MS2] P only for $a_0 \gtrsim 0.3$ AU.

To verify that our results are not dependent on the choice of a_1, we now consider the relative probabilities for scenarios 1 and 2 over a large grid in a_0-a_1 space. To simplify the presentation of the results, we plot the normalized cross section for each outcome, $\sigma/\pi(a_0 + a_1)^2$, as a function of a_1/a_0, as shown in Figure 8; hence the multivalued nature of the cross sections. For simplicity, all interactions were performed with $v_\infty = 5$ km s^{-1}, since the velocity-dependent rate peaks at this value. It is clear from the figure that as long as $a_1 \gtrsim a_0$, which is quite reasonable on physical grounds, scenario 2 is the most probable. For the physically most reasonable value of $a_1/a_0 \approx 10$, scenario 2 is more probable by more than an order of magnitude over scenario 1.

Now that we have confirmed the preferred formation scenario, we consider the orbital parameters of the hierarchical triple system formed. Figure 9 shows the cumulative distribution of the center-of-mass velocity of the triple system after the exchange interaction for the cases with $a_0 = 0.1$ AU (*solid lines*) and $a_0 = 1$ AU (*dotted lines*) for several values of v_∞, from 1 km s^{-1} (*leftmost line*) to 15 km s^{-1} (*rightmost line*). The triple system appears to suffer a recoil of ∼3 km s^{-1}, which is clearly not enough to eject it from the cluster (which would require ≈15 km s^{-1}), but may be enough to eject it from the core. Figures 10 and 11 show the cumulative distributions of the outer semimajor axis, a_{out}, and the eccentricity, e_{out}, respectively, with the same convention for the line types as in Figure 9. The outer semimajor axis is clearly not particularly dependent on either a_0 or v_∞, with a peak at ∼10 AU. The outer eccentricity, on the other hand, while not particularly dependent on v_∞, is strongly dependent on a_0. For $a_0 = 0.1$ AU the eccentricity distribution is roughly thermal, with the cumulative
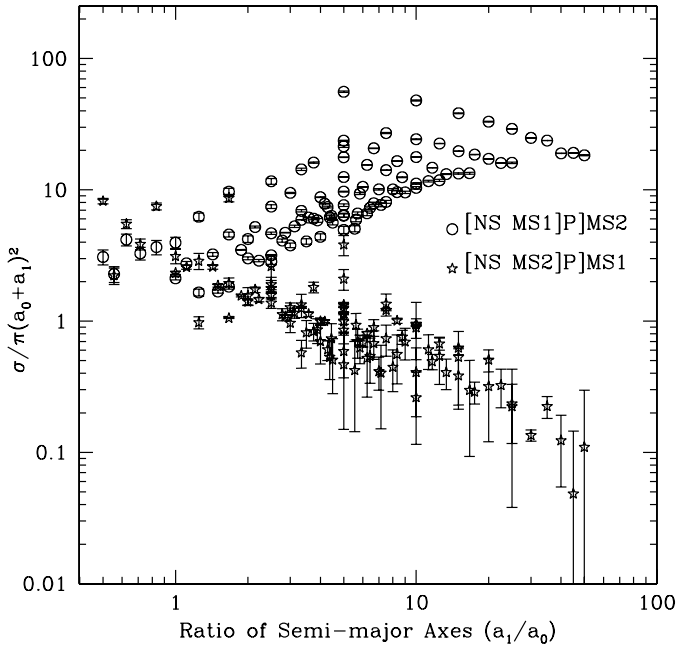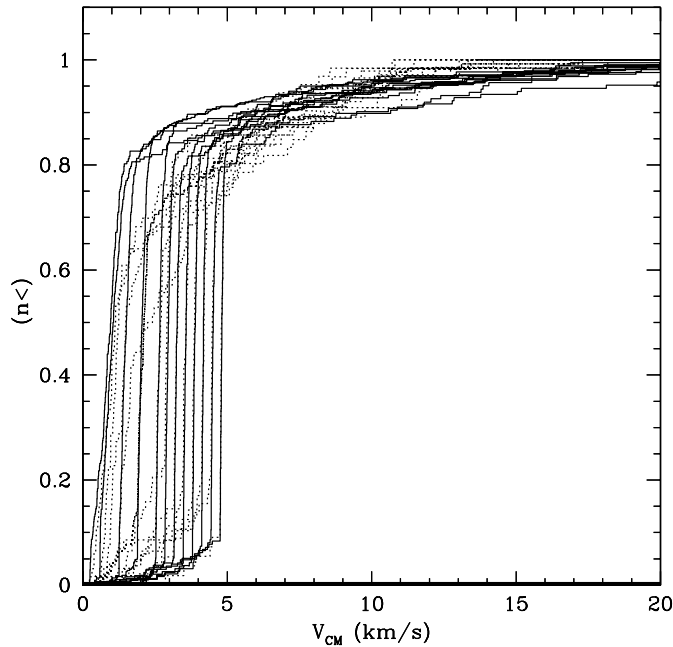
Fig. 8.—Normalized cross section, $\sigma/\pi(a_0 + a_1)^2$, for PSR B1620$-$26 formation scenarios 1 (*stars*) and 2 (*circles*) as a function of a_1/a_0, where a_0 is the initial semimajor axis of the neutron star binary and a_1 is that of the planet binary. The cross sections are calculated over a large grid in a_0-a_1 space; hence, their multivalued nature as a function of a_1/a_0. All interactions were performed with $v_\infty = 5$ km s^{-1}, since the velocity-dependent rate peaks at this value. It is clear from the figure that as long as $a_1 \gtrsim a_0$, which is quite reasonable on physical grounds, scenario 2 is the most likely.

Fig. 10.—Cumulative distribution of the outer semimajor axis, $a_{\rm out}$, for the putative PSR B1620$-$26 triple system formed in scenario 2. Line conventions and initial conditions are the same as in Fig. 9.

distribution $\propto e_{\rm out}^2$. For $a_0 = 1$ AU the eccentricity distribution is flatter, with more systems at lower eccentricity. This result suggests that of the two, $a_0 = 1$ AU is the favored value for the NS binary semimajor axis, since we know from observations that the outer eccentricity is rather low, with $e_{\rm out} \sim 0.2 \pm 0.1$ (Sigurdsson & Thorsett 2005). In Figure 12 we show the cumulative distribution of the inner binary semimajor axis, $a_{\rm in}$, with the same convention for the line types as in the previous figures. Confirming our earlier assumption, the inner binary clearly behaves as a single dynamical unit, with the distributions for the final values strongly

Fig. 9.—Cumulative distribution of the center-of-mass velocity of the putative PSR B1620$-$26 triple system after the exchange interaction in scenario 2, for the cases $a_0 = 0.1$ AU (*solid lines*) and $a_0 = 1$ AU (*dotted lines*) for several values of v_∞, from 1 km s^{-1} (*leftmost lines*) to 15 km s^{-1} (*rightmost lines*). In both cases we set $a_1 = 5$ AU. The triple system appears to suffer a recoil of $\sim$3 km s^{-1}, which is clearly not enough to eject it from the cluster (which would require $\approx$15 km s^{-1}), but may be enough to displace it significantly away from the core.

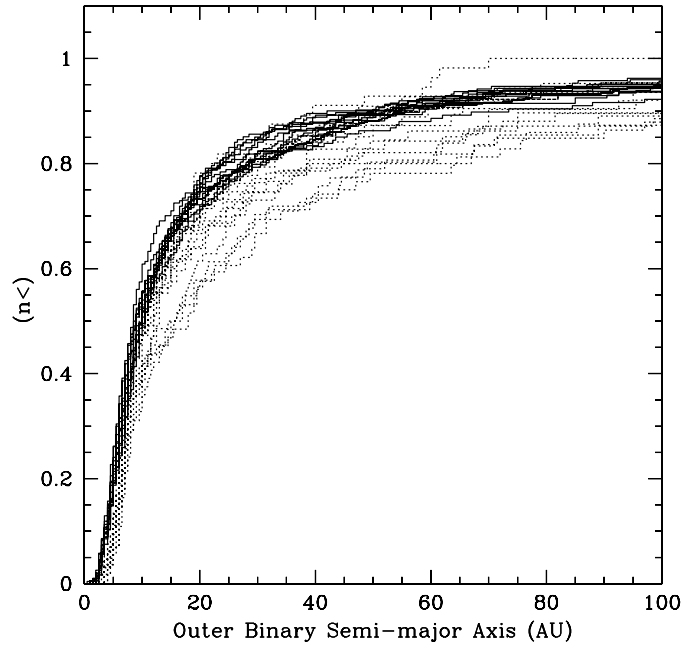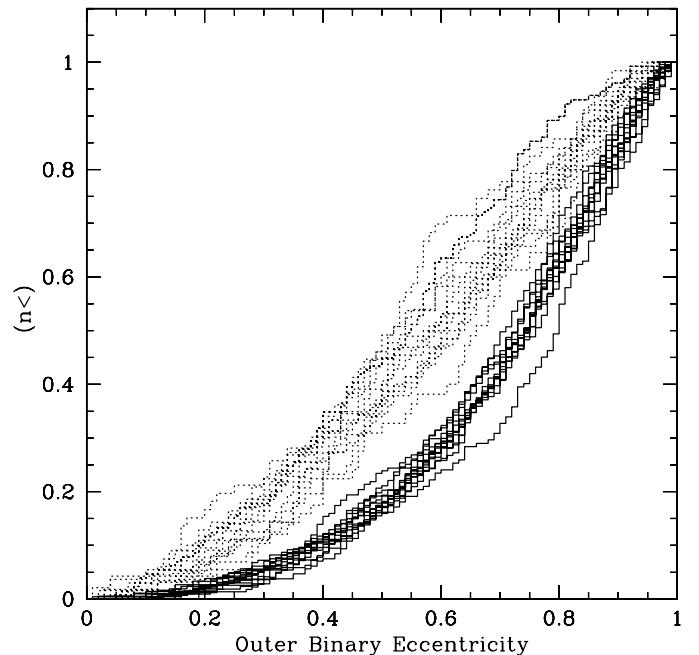Fig. 11.—Cumulative distribution of the outer eccentricity, $e_{\rm out}$, for the putative PSR B1620$-$26 triple system formed in scenario 2. Line conventions and initial conditions are the same as in Fig. 9.
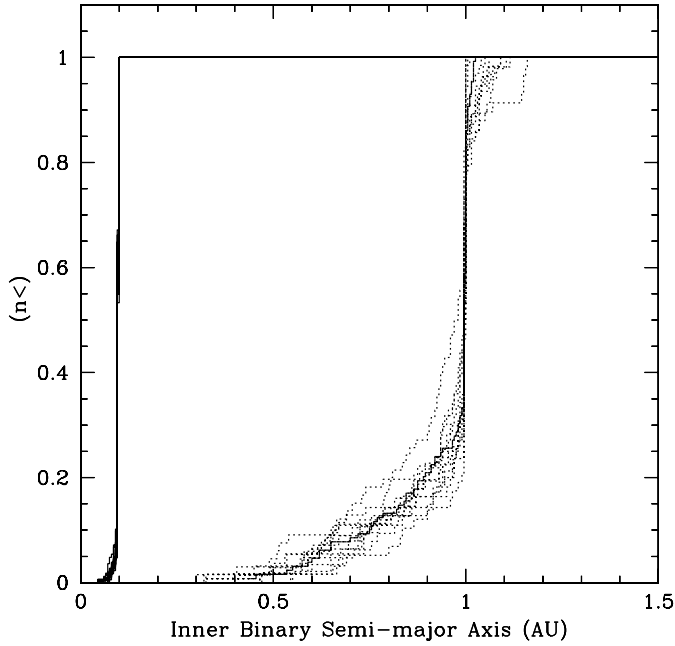
Fig. 12.—Cumulative distribution of the inner semimajor axis, a_{in}, for the putative PSR B1620−26 triple system formed in scenario 2. Line conventions and initial conditions are the same as in Fig. 9.

peaked around their initial values, and with very minimal dependence on v_∞.

6.2. *Evolution of the Hierarchical Triple Due to Mass Transfer*

In scenario 2, the hierarchical triple system formed via the dynamical interaction is not the planetary system we see today in M4, but merely its progenitor. In this section we calculate the effects on the triple system due to mass transfer in the inner binary as the main-sequence star ascends the red giant branch and apply the results to the ensemble of triple systems formed in our scattering interactions. We assume slow isotropic mass loss and that during this process the eccentricities remain invariant (Rasio et al. 1992). For the sake of simplifying the calculation, we also assume that the inner and outer eccentricities are zero. Since the outer orbit carries so little angular momentum ($\sim0.4\%$ of the total angular momentum of the triple system), we neglect angular momentum coupling between the two orbits and treat them as two separate binaries during the mass transfer.

The angular momentum of the inner orbit is given by

$$L_{in} = M_{NS}M_{MS1}\left(\frac{Ga_{in}}{M_{in}}\right)^{1/2},\qquad(24)$$

where $M_{in} = M_{NS} + M_{MS1}$, M_{NS} and M_{MS1} are the masses of the NS and the WD progenitor star, respectively, and a_{in} is the semimajor axis of the inner binary. Similarly, the angular momentum of the outer orbit is given by

$$L_{out} = M_{in}M_P\left(\frac{Ga_{out}}{M_T}\right)^{1/2},\qquad(25)$$

where $M_T = M_{in} + M_P$, M_P is the mass of the planet, and a_{out} is the semimajor axis of the outer orbit. If we take the logarithm of both sides and differentiate, we get

$$\frac{\delta L_{in}}{L_{in}} = \frac{\delta M_{NS}}{M_{NS}} + \frac{\delta M_{MS1}}{M_{MS1}} + \frac{1}{2}\frac{\delta a_{in}}{a_{in}} - \frac{1}{2}\frac{\delta M_{in}}{M_{in}}\qquad(26)$$
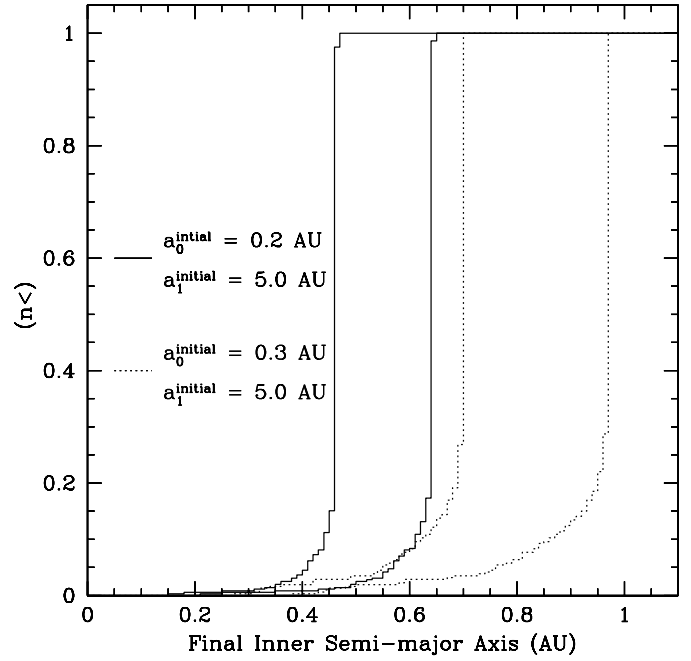

Fig. 13.—Cumulative distribution of the inner binary semimajor axis of the putative PSR B1620−26 triple system after mass transfer. The solid lines represent the case with $a_0 = 0.2$ AU; in other words, the NS-MS1 semimajor axis was 0.2 AU before the scattering interaction. The dotted lines represent the case with $a_0 = 0.3$ AU. In both cases we set $a_1 = 5$ AU and $v_\infty = 5$ km s^{-1}. For each set of lines, the rightmost line represents completely nonconservative mass transfer ($\beta = 0$), while the leftmost line represents completely conservative mass transfer ($\beta = 1$).

and

$$\frac{\delta L_{out}}{L_{out}} = \frac{\delta M_{in}}{M_{in}} + \frac{\delta M_P}{M_P} + \frac{1}{2}\frac{\delta a_{out}}{a_{out}} - \frac{1}{2}\frac{\delta M_T}{M_T}\qquad(27)$$

for differential changes in the inner and outer orbits.

In the mass transfer process, we assume that the mass lost from MS1 gets channeled into an accretion disk around the NS and that any mass lost from the system is lost from the accretion disk with the characteristic angular momentum of the NS (see, e.g., Podsiadlowski et al. 2002). This implies that

$$\delta L_{in} = a_{in}^2\frac{M_{MS1}^2}{M_{in}^2}\Omega_{in}\delta M_{in},\qquad(28)$$

where Ω_{in} is the orbital velocity of NS, given by

$$\Omega_{in} = \left(\frac{GM_{in}}{a_{in}^3}\right)^{1/2}.\qquad(29)$$

Similarly, as mass is lost from the inner binary in the mass transfer process, the angular momentum of the outer binary will change according to

$$\delta L_{out} = a_{out}^2\frac{M_P^2}{M_T^2}\Omega_{out}\delta M_T,\qquad(30)$$

where Ω_{out} is the orbital angular velocity of the inner binary in the outer orbit and is given by

$$\Omega_{out} = \left(\frac{GM_T}{a_{out}^3}\right)^{1/2}.\qquad(31)$$
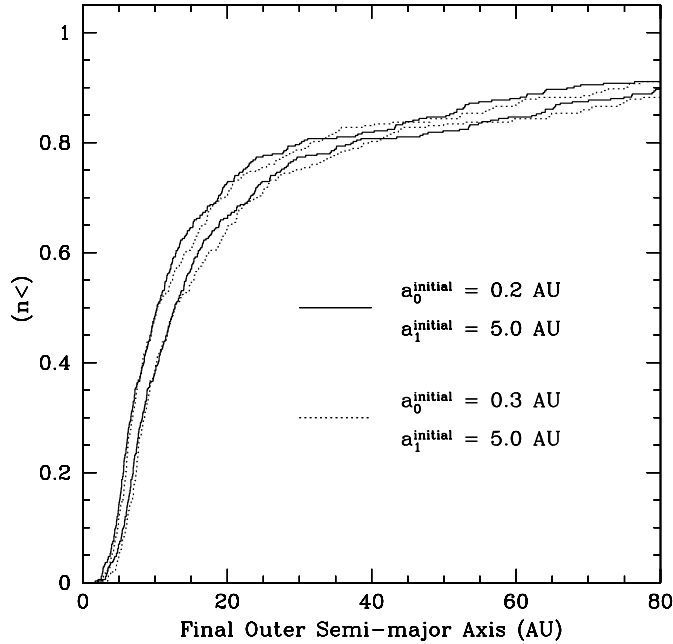
Fig. 14.—Cumulative distribution of the outer semimajor axis of the putative PSR B1620−26 triple system after mass transfer for the cases $a_0 = 0.2$ AU (*solid lines*) and $a_0 = 0.3$ AU (*dotted lines*). Line conventions and initial conditions are the same as in Fig. 13.

We parameterize the mass loss by defining β as the fraction of mass lost from MS1 that is accreted by the NS, so that $\delta M_{NS} = -\beta \delta M_{MS1}$ and $\delta M_{in} = (1 - \beta)\delta M_{MS1}$. Note that with our conventions $\delta M_{MS1} < 0$. By combining equations (24)–(31), converting the δ quantities to differentials, and integrating, we find (Podsiadlowski et al. 2002)

$$\frac{a'_{in}}{a_{in}} = \left(\frac{M'_{MS1}}{M_{MS1}}\right)^{-2} \left(\frac{M'_{NS}}{M_{NS}}\right)^{-2/\beta} \left(\frac{M'_{in}}{M_{in}}\right)^{-1} \quad \text{for } 0 < \beta \leq 1, \tag{32}$$

$$\frac{a'_{in}}{a_{in}} = \left(\frac{M'_{MS1}}{M_{MS1}}\right)^{-2} \left(\frac{M'_{in}}{M_{in}}\right)^{-1} \exp\left[2\left(\frac{M'_{MS1} - M_{MS1}}{M_{NS}}\right)\right] \quad \text{for } \beta = 0, \tag{33}$$

$$\frac{a'_{out}}{a_{out}} = \left(\frac{M'_T}{M_T}\right)^{-1} \quad \text{for all } \beta. \tag{34}$$

We can apply the expressions in equations (32)–(34) to the ensemble of triple systems formed via scenario 2 to determine their properties after mass transfer. Figure 13 shows the cumulative distribution of the inner binary semimajor axis after mass transfer. The solid lines represent $a_0 = 0.2$ AU; in other words, the NS-MS1 semimajor axis was 0.2 AU before the scattering interaction. The dotted lines represent the case in which $a_0 = 0.3$ AU. In both cases we set $a_1 = 5$ AU and $v_\infty = 5$ km s^{-1}. For each set of the lines, the rightmost line represents completely nonconservative mass transfer ($\beta = 0$), while the leftmost line represents completely conservative mass transfer ($\beta = 1$). Figure 14 shows the cumulative distribution of the outer semimajor axis for the cases with $a_0 = 0.2$ and 0.3 AU. Line types are as in Figure 13. If we compare the distributions of the inner semimajor axis after the scattering interaction in Figure 12 with those after mass transfer in Figure 13, we see that the effect of mass transfer is to create a spread in the distribution that is of order the initial value.

From observations we know the period of the inner orbit to be 191 days, which corresponds to a semimajor axis of ≈ 0.8 AU (Sigurdsson & Thorsett 2005). From this figure we see that we can quite reasonably create such a system with $a_0 \approx 0.3$ AU for a wide range in the mass transfer parameter β. From Figure 14 we see that the distribution of the outer semimajor axis after mass transfer is much broader. Although the peak in the distribution appears to occur around 5–10 AU, it is quite plausible to form a system with an outer semimajor axis of 20 AU, as we observe for the system today.

7. SUMMARY AND CONCLUSIONS

We have studied in detail dynamical scattering interactions between star-planet systems and other single stars, tabulating analytical cross sections for all possible outcomes of the scattering encounter and confirming them with numerical experiments (as shown in Fig. 3). In the scattering of planetary systems (or wide mass ratio binaries in general), there are two characteristic velocities in the problem (as shown in Fig. 1): the critical velocity v_c, which is the value of v_∞ for which the total energy of the three-body system is zero, and v_{orb}, the orbital speed in the binary. For a mass ratio of $q \lesssim 10^{-3}$, the two characteristic velocities differ by more than an order of magnitude, opening up a region in parameter space in which the nature of the scattering process is fundamentally different from what occurs in comparable-mass encounters. For $v_c < v_\infty < v_{orb}$, two outcomes dominate the cross section with roughly equal weight: ionization, which destroys the planetary system, and exchange of the incoming star for the planet's original host star. Thus, in this region, which does not exist for comparable-mass systems, there is a significant probability that a planetary system undergoing a strong dynamical encounter will survive, albeit with a new host star. Since in the past workers in the field have typically taken v_c as the velocity above which planetary systems are predominantly destroyed, this implies a greater survivability of planetary systems in dense stellar environments than has been predicted in some cases, as the characteristic lifetime plotted in Figure 6 shows.

We have also numerically determined the location of the hard-soft boundary for planetary systems, and we find that it lies at $v_\infty \approx 0.75 v_c$. In other words, interactions with $v_\infty < v_c$ in which the binary survives (e.g., via exchange) typically harden (a decreases), while for $v_\infty > v_c$ surviving binaries soften (a increases). However, this simple statement belies the rich structure of the parameter space. In particular, for $v_c < v_\infty < v_{orb}$, although the surviving binary typically softens, it softens by only a small amount, increasing its semimajor axis by only $\sim 25\%$, as shown in Figure 5. Its final eccentricity, of course, is uncorrelated with the initial value, taking on a thermal distribution ($dP/de = 2e$). Only for $v_\infty > v_{orb}$ does the binary soften by a large amount; that is, if it is not destroyed completely, which is the overwhelmingly dominant outcome for this region of parameter space.

We have briefly explored the implications of our results. As mentioned above, the main implication is that the minimum size of a planetary system that will likely be destroyed as a result of dynamical interactions in dense stellar environments is larger than has previously been assumed. For a stellar environment of a given velocity dispersion and density, this limit can be read almost directly off of Figure 6. By applying our results to the observational campaigns searching for hot Jupiters in 47 Tuc via stellar transits, we find that the planetary systems that the Gilliland et al. (2000) observations were sensitive to would have in fact survived to the present day. This bolsters the conclusion drawn by Weldrake et al. (2005) that it is not dynamics that is

responsible for the lack of hot Jupiters detected in 47 Tuc, but rather may be metallicity-dependent effects. Looking toward the future, we predict that a MSP-planet binary may likely be detected via pulsar timing in the supersolar-metallicity cluster Terzan 5, with a semimajor axis of $\sim$0.1 AU.

Since we recognized that the planetary system PSR B1620$-$26 in the globular cluster M4 lies in the "intermediate" region of parameter space, we have performed a detailed numerical study of the possible scenarios in which it may have formed. By calculating cross sections and interaction rates and treating the effects of mass transfer in the inner binary, we conclude that the scenario in which a NS-MS binary exchanges as a single dynamical unit into the planetary system for the planet's original host star (similar to the scenario of Ford et al. 2000) is strongly favored over that of Sigurdsson et al. (2003), in which the exchange interaction involves ejecting the original NS binary companion, with the planet's host star exchanging into it. This statement is quantified in Figure 8 for a wide range of initial binary semimajor axes.

Our general analysis (§§ 2$-$5) does not consider the effects of direct physical collisions between objects (e.g., MS stars and planets), which may play an important role when the ratio of stellar size to binary semimajor axis is $\gtrsim$0.01 (Fregeau et al. 2004). However, our code accurately treats physical collisions, and we have allowed for collisions in our analysis of PSR B1620$-$26 in § 6, as shown in the cross sections of Figure 7. We have not looked at the ejection speeds of the planets in encounters that destroy the planetary system. This topic has already been studied in detail using N-body methods (Smith & Bonnell 2001; Hurley & Shara 2002).

Since our results assume point-mass particles, they are applicable to systems of any mass, as long as the mass ratio in the binary is relatively small ($\lesssim$0.1) and the incoming object and the heaviest object in the binary are of comparable mass. We have not yet explored the application to scenarios involving, for example, intermediate-mass black holes and supermassive black holes, stars and intermediate-mass black holes, and planetesimals and planets. Our results may also have limited application to wide mass ratio binaries containing more than one light body, as long as the total mass in light objects is significantly less than the host mass, and the orbits of the light objects are not so strongly coupled that they transmit perturbations on timescales comparable to the orbital period.

REFERENCES

Backer, D. C. 1993, in ASP Conf. Ser. 36, Planets around Pulsars, ed. J. A. Phillips, S. E. Thorsett, & S. R. Kulkarni (San Francisco: ASP), 11
Basri, G. 2004, Nature, 430, 24
Beer, M. E., King, A. R., & Pringle, J. E. 2004, MNRAS, 355, 1244
Bonnell, I. A., Smith, K. W., Davies, M. B., & Horne, K. 2001, MNRAS, 322, 859
Butler, R. P., Vogt, S. S., Marcy, G. W., Fischer, D. A., Henry, G. W., & Apps, K. 2000, ApJ, 545, 504
Davies, M. B., & Sigurdsson, S. 2001, MNRAS, 324, 612
Fischer, D. A., & Valenti, J. 2005, ApJ, 622, 1102
Ford, E. B., Joshi, K. J., Rasio, F. A., & Zbarsky, B. 2000, ApJ, 528, 336
Fregeau, J. M., Cheung, P., Portegies Zwart, S. F., & Rasio, F. A. 2004, MNRAS, 352, 1
Gehrels, N. 1986, ApJ, 303, 336
Gilliland, R. L., et al. 2000, ApJ, 545, L47
Harris, W. E. 1996, AJ, 112, 1487
Heggie, D., & Hut, P. 2003, The Gravitational Million-Body Problem: A Multidisciplinary Approach to Star Cluster Dynamics (Cambridge: Cambridge Univ. Press)
Heggie, D. C. 1975, MNRAS, 173, 729
Heggie, D. C., Hut, P., & McMillan, S. L. W. 1996, ApJ, 467, 359
Hills, J. G. 1975, AJ, 80, 809
———. 1984, AJ, 89, 1559
———. 1990, AJ, 99, 979
Hills, J. G., & Dissly, R. W. 1989, AJ, 98, 1069
Hurley, J. R., & Shara, M. M. 2002, ApJ, 565, 1251

Hut, P. 1983, ApJ, 268, 342
Hut, P., & Bahcall, J. N. 1983, ApJ, 268, 319
Kenyon, S. J., & Bromley, B. C. 2004, Nature, 432, 598
Kobayashi, H., Ida, S., & Tanaka, H. 2005, Icarus, 177, 246
Konacki, M. 2005, Nature, 436, 230
Laughlin, G., & Adams, F. C. 1998, ApJ, 508, L171
McMillan, S. L. W., & Hut, P. 1996, ApJ, 467, 348
Morbidelli, A., & Levison, H. F. 2004, AJ, 128, 2564
Pfahl, E. 2005, ApJ, 635, L89
Podsiadlowski, P., Rappaport, S., & Pfahl, E. D. 2002, ApJ, 565, 1107
Portegies Zwart, S. F., & McMillan, S. L. W. 2005, ApJ, 633, L141
Portegies Zwart, S. F., McMillan, S. L. W., Hut, P., & Makino, J. 2001, MNRAS, 321, 199
Ransom, S. M., Hessels, J. W. T., Stairs, I. H., Freire, P. C. C., Camilo, F., Kaspi, V. M., & Kaplan, D. L. 2005, Science, 307, 892
Rasio, F. A., Shapiro, S. L., & Teukolsky, S. A. 1992, A&A, 256, L35
Sigurdsson, S. 1992, ApJ, 399, L95
Sigurdsson, S., Richer, H. B., Hansen, B. M., Stairs, I. H., & Thorsett, S. E. 2003, Science, 301, 193
Sigurdsson, S., & Thorsett, S. E. 2005, in ASP Conf. Ser. 328, Binary Radio Pulsars, ed. F. A. Rasio & I. H. Stairs (San Francisco: ASP), 213
Smith, K. W., & Bonnell, I. A. 2001, MNRAS, 322, L1
Thorsett, S. E., Arzoumanian, Z., Camilo, F., & Lyne, A. G. 1999, ApJ, 523, 763
Weldrake, D. T. F., Sackett, P. D., Bridges, T. J., & Freeman, K. C. 2005, ApJ, 620, 1043